

Crystal Structure of the Free Radical Intermediate of Pyruvate:Ferredoxin Oxidoreductase

Eric Chabrière,^{1,3} Xavier Vernède,¹ Bruno Guigliarelli,² Marie-Hélène Charon,¹ E. Claude Hatchikian,² Juan C. Fontecilla-Camps^{1*}

In anaerobic organisms, the decarboxylation of pyruvate, a crucial component of intermediary metabolism, is catalyzed by the metalloenzyme pyruvate:ferredoxin oxidoreductase (PFOR) resulting in the generation of low potential electrons and the subsequent acetylation of coenzyme A (CoA). PFOR is the only enzyme for which a stable acetyl thiamine diphosphate (ThDP)-based free radical reaction intermediate has been identified. The 1.87 Å-resolution structure of the radical form of PFOR from *Desulfovibrio africanus* shows that, despite currently accepted ideas, the thiazole ring of the ThDP cofactor is markedly bent, indicating a drastic reduction of its aromaticity. In addition, the bond connecting the acetyl group to ThDP is unusually long, probably of the one-electron type already described for several cation radicals but not yet found in a biological system. Taken together, our data, along with evidence from the literature, suggest that acetyl-CoA synthesis by PFOR proceeds via a condensation mechanism involving acetyl (PFOR-based) and thyl (CoA-based) radicals.

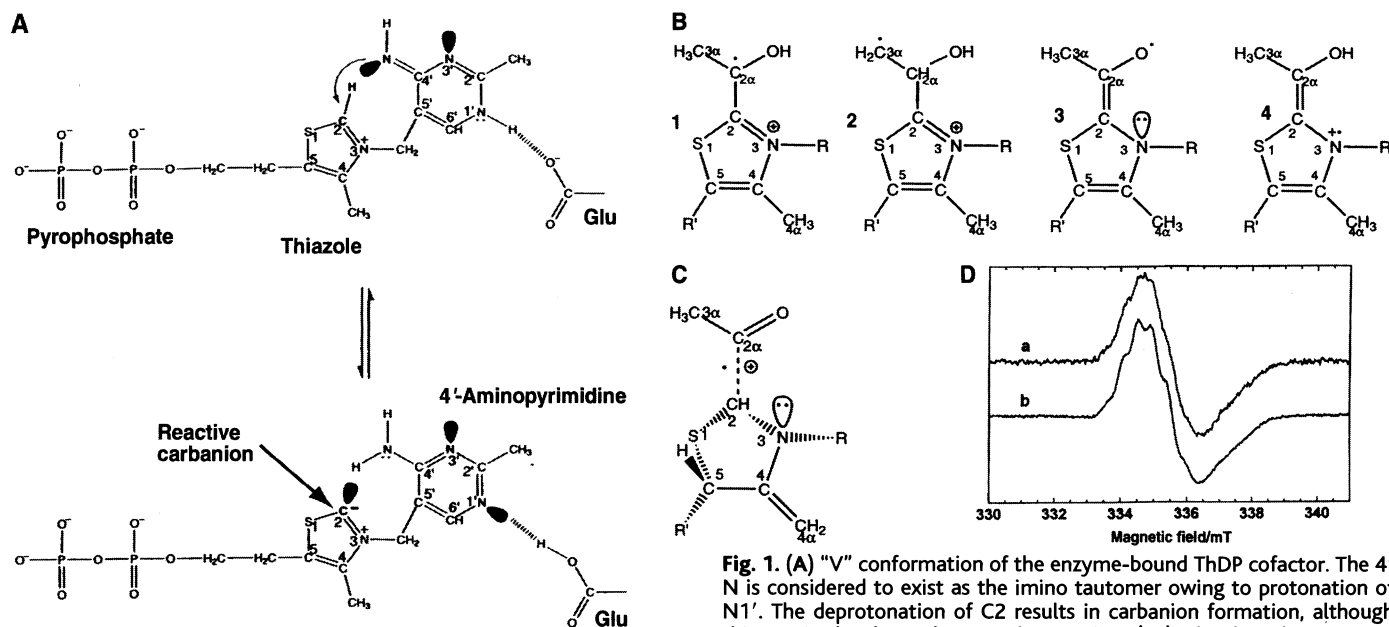
dehydrogenase (PDH) and use NAD as the electron acceptor (1, 2). Alternatively, when pyruvate is oxidized by anaerobic organisms, electrons are transferred to acceptors with more negative potentials than NAD, such as ferredoxins (Fd). The corresponding reaction, $\text{CH}_3\text{-CO-COO}^- + \text{Fd}_{\text{ox}} + \text{CoA} \leftrightarrow \text{CH}_3\text{-CO-CoA} + \text{Fd}_{\text{red}} + \text{CO}_2$, is catalyzed by the [4Fe4S] cluster-containing pyruvate:ferredoxin oxidoreductase (PFOR) (3). Although both PFOR and PDH are thiamine diphosphate (ThDP)-containing enzymes, only the former can carry out the reverse reaction, that is, the reductive carboxylation of acetyl-CoA to yield pyruvate. This reaction constitutes the basis for CO_2 fixation in green photosynthetic and acetogenic bacteria (4) and in methanogens (5). Pyruvate synthesis by PFOR is thought to have taken over the primordial double carbonylation reactions, leading to pyruvic acid synthesis postulated in the

¹Laboratoire de Cristallographie et Cristallogénèse des Protéines, Institut de Biologie Structurale Jean-Pierre Ebel, Commissariat à l'Energie Atomique, Université Joseph Fourier, CNRS, 41, rue Jules Horowitz, 38027 Grenoble Cedex 1, France. ²Unité de Bioénergétique et Ingénierie des Protéines, Institut de Biologie Structurale et Microbiologie, CNRS, 31, chemin J. Aiguier, 13402 Marseille, France. ³Laboratoire de Cristallographie et Modélisation des Matériaux Minéraux et Biologiques, Unité Mixte de Recherche 7036 CNRS, Université Henri Poincaré, Nancy 1B.P. 239, 54506 Vandœuvre-les-Nancy, France.

*To whom correspondence should be addressed. E-mail: juan@lccp.ibs.fr

The oxidative decarboxylation of pyruvate is coupled, in most organisms, to the reduction of low potential electron carriers and the subsequent formation of an energy-rich thio-

ester bond between the nascent acyl group and coenzyme A (CoA). In mitochondria and respiratory eubacteria, these reactions are catalyzed by the multienzyme complex pyruvate



is represented with the conventional C4-C5 double bond. (B) Postulated radical species of the hydroxyethyl-ThDP intermediate (R = 5'-methyl, 4'-aminopyrimidine; R' = pyrophosphate), models 1 to 4 proposed by Barletta *et al.* (31), Docampo *et al.* (22), Menon and Ragsdale (12), and Bock *et al.* (20), respectively. These models require a planar conformation for the thiazolium moiety; (C) the model proposed in this work on the basis of crystallographic analysis. The unpaired electron and the positive charge are depicted between C2 and C2 α as is customary for one-electron bonds (27). The proton is assumed to be bound to C2. As indicated in the text, after C2-C2 α fragmentation, the reactive species is likely to be an acetyl radical with significant spin density at C2 α . (D) EPR spectra of PFOR incubated with pyruvate at pH = 9.0 (14). (a) Crystals, 10 scans; (b) protein in solution, 1 scan. Both spectra display a signal centered at $g = 2.005$ that exhibits line widths and hyperfine structures identical to those already reported for the acetyl-ThDP radical species of several PFORs (13, 14, 24).

“iron-sulfur world” theory of the origin of life (6, 7). Other ThDP-containing enzymes are involved in 2-oxoacid decarboxylations of both the nonoxidative and oxidative types. Examples of the first class are pyruvate decarboxylase and benzoyl-formate decarboxylase; a related enzyme is transketolase, which transfers a ketol group from a keto-sugar to an aldose. In addition to PFOR and PDH, oxidative decarboxylations are also catalyzed by pyruvate oxidase. PFORs can have different oligomeric structures, but they are all phylogenetically closely related (8, 9).

Hypotheses concerning the catalytic mechanism of ThDP-containing enzymes in general (10) are based on two observations: that the enzyme-bound ThDP adopts the “V” configuration, bringing the 4' amino group of the aminopyrimidine (amino-Pyr) ring close to the C2 carbon of the thiazolium ring (Fig. 1A) and that hydrogen bonding of the carboxylate group from a glutamate residue to N1' of the amino-Pyr increases the basic nature of the 4' position by generating the 4'-imino tautomer. Accordingly, catalysis is thought to proceed through (i) the generation of a carbanion by proton extraction from C2 (probably by the 4'-imino group) (11); (ii) protonation of the carbonyl oxygen of the

substrate (probably from the 4'-imino species) (11) and attack of the carbonyl carbon by the C2 carbanion; (iii) cleavage, in the case of pyruvate, of the C1 α -C2 α bond followed by (iv) release of CO₂ and generation of the enamine (or the equivalent C2 α -carbanion) species. From this point on, the reaction mechanism varies depending on the enzyme. In PFORs, one of the two electrons involved in the reaction is subsequently transferred from the cofactor to one of the [4Fe4S] cluster [cluster A (12)] generating a substituted ThDP-based radical species (Fig. 1, B and C). This radical intermediate can be characterized when the reaction is carried out in the absence of CoA because, under those conditions, the second electron is not readily removed from the active site (13). There has been some controversy concerning the generality of the radical species in PFORs. In this regard, Menon and Ragsdale have proposed that the radical adduct is an intermediate species in all PFORs but may decay if the sample is not frozen rapidly enough before electron paramagnetic resonance (EPR) spectroscopic analyses (12). The free radical species of the homodimeric PFOR ($M_r = 266$ kD) from *Desulfovibrio africanus*, an anaerobic sulfate-reducing bacterium, is unusually

stable, a property that may be related to the relative oxygen insensitivity of the enzyme (14). PFORs belong to an increasing number of enzymes that are reported to use a radical-based mechanism. Spectroscopic evidence for such mechanisms has been well documented for the tyrosyl radical of aerobic ribonucleotide reductase (RNR) (15), and the 5'-deoxyadenosyl radical of pyruvate formate-lyase, biotin synthase, and anaerobic ribonucleotide reductase generated either from S-adenosylmethionine (SAM) or from adenosylcobalamin (16). In both systems, radical formation is initiated by one electron donated from a dinuclear Fe center in RNR, an [Fe-S] cluster in SAM-dependent enzymes, or the homolytic cleavage of a Co-C bond in adenosylcobalamin-containing pro-

Table 1. Crystallographic analysis. Crystals of PFOR were grown aerobically from micro-seeds as described (17) except that the buffer was 100 mM Tris-maleate, pH 9.0. The crystallization plates were subsequently transferred to a glove box under 10% H₂ and 90% N₂, and their reservoir solutions were bubbled with this gas mixture for 30 s. This procedure was sufficient to remove any detectable amounts of oxygen from the solutions. A solution (2 μ l) containing 15% (v/v) PEG 6000 and 200 mM pyruvate in the crystallization buffer was slowly added to the 2- μ l crystallization drop. The same pyruvate concentration was added to the cryoprotecting solutions. After a 15-hour soak, the crystals were flash-cooled in liquid propane inside the glove box (33) and stored in liquid nitrogen. Data were collected from one such crystal at the ID14 EH3 beam line of the European Synchrotron Radiation Facility. Subsequent data reduction was carried out using MOSFLM and programs from the CCP4 suite (34). The structure was solved by molecular replacement using X-Plor (35) and the native PFOR atomic coordinates (PDB accession code 1b0p) and subsequently refined with the Crystallography and NMR System (CNS) (36). rmsd, root mean square deviation.

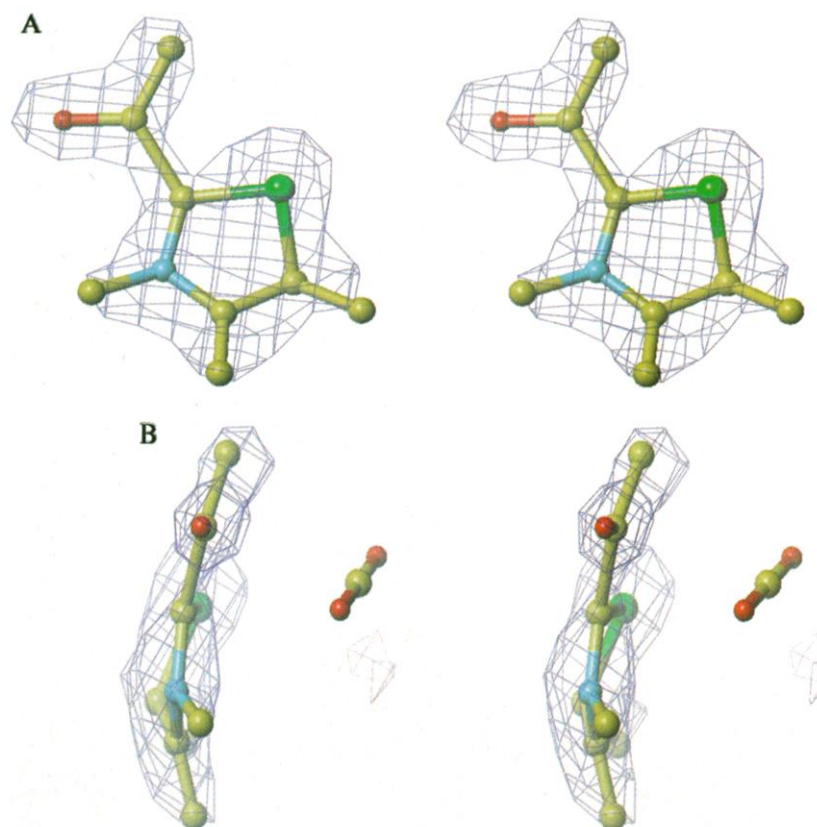


Fig. 2. Stereo pairs of the omit 1.87 Å-resolution Fourier maps of the thiazole radical adduct of molecule A (Table 1). (A and B) Electron density maps calculated after removing 20% of the corresponding native structure contribution from both phases and structure factor calculations. (18). The maps have been contoured at the 3 σ level. This figure was prepared using Turbo-Frodo (38).

Parameter	Value
<i>Data collection</i>	
Space group	P 2 ₁ 2 ₁ 2 ₁
Unit cell parameters (Å)	a = 86.1, b = 145.8, c = 210.3
Wavelength (Å)	1.005
Resolution (Å)	1.87
Redundancy (last bin)	3.6
Completeness (last bin) (%)	94.4 (97.3)
I/ $\Sigma(I)$ (last bin)	5.8 (1.4)
R _{sym} (last bin) (%)*	8.4 (29.3)
<i>Refinement statistics</i>	
Resolution range (Å)	30–1.87
No. of unique reflections	20,0561
R _{work} /R _{free} (%)	18.3/23.8
No. of protein atoms	20,783
Average B-factor (Å ²), molecule A, molecule B	31.7, 27.2
No. of water molecules	1912
rmsd bond length (Å)	0.0014
rmsd bond angle (°)	1.9

*R_{sym} = $\sum |I - \langle I \rangle| / \sum I$, where the summation is over all symmetry equivalent reflections.

teins. Subsequently, free radical formation is propagated through the enzyme by hydrogen atom abstraction, either from the substrate or from glycine or cysteine residues, resulting in the corresponding glycylyl or thiyl radicals (16). In PFORs, radical generation results from one electron abstraction, and the radical species does not propagate through the enzyme. Relative to its tyrosinyl and glycylyl counterparts, the acetyl-ThDP radical, being a reaction intermediate, should be intrinsically less stable. However, radical stability in PFORs seems to be significantly increased by the ThDP cofactor and the protein environment which shelters it from nonspecific reactions. We conclude that PFORs have a radical-based mechanism that differs appreciably from the others reported so far.

We have recently solved the structure of the uncomplexed *D. africanus* PFOR at 2.3 Å resolution using crystals grown at pH 6.2 (17). Here, we report on the 1.87 Å-resolution, active-site structure of this PFOR solved from crystals soaked with pyruvate

at pH 9.0 in an anaerobic glove box (Table 1) (18). Under these conditions, the substrate gets decarboxylated, and a stable radical species is present in the crystalline enzyme with an occupancy of about 1.6 spins for the PFOR dimer, as indicated by EPR measurements (18) (Fig. 1D). This report on the structure of a putative catalytic intermediate of a ThDP-containing enzyme describes one of the few cases where a radical species has been characterized in a protein crystal in general (19), and substantial conformational changes are observed. As expected, these active site changes are the only significant differences between the structure presented here and the native PFOR. Superposition of the radical and native forms into the electron density calculated after crystallographic refinement suggested that, as indicated by the EPR analysis, a fraction of the PFOR molecules had not reacted [Web fig. 1 (18)]. Indeed, omit maps that were calculated to include a 20% native thiazolium contribution to

phases and structure factors show a very good fit of the radical thiazole to the electron density (Fig. 2). The positions of the bound ThDP acetyl and CO₂ groups are indicated in Fig. 3A. The C2 α atom of the acetyl-ThDP lies about 3.1 Å away from the carbon atom of CO₂, suggesting that only minor rearrangements have occurred upon cleavage of the substrate C1 α -C2 α bond, as expected from the minimal-movement, maximum-orbital overlap principle (20). This unusual arrangement at the active site with a tightly bound CO₂ would also be required for an intermediate state in the reverse reaction, that is, the synthesis of pyruvate from acetyl-CoA and CO₂.

The most surprising observation, however, is the drastic reduction of the aromaticity of the substituted ThDP thiazole ring, a process generally considered to be unfavorable (21). This significant loss of aromaticity may have resulted from the ketonization of either the enamine intermediate (21), or the radical species (Fig. 4). In our electron density maps, the ring bends along a line connecting N3 to C5, apparently because of the, at least partial, sp³ hybridization of these two atoms (Fig. 2, A and B). In addition, the pyruvate-derived group does not lie in the plane defined by S1, C2, and C5, and the C2-C2 α bond is unusually long (see below). The most consistent proposition for the stereochemistry of thiazole in the radical species implies the tautomerization of the double bond between C5 and C4 to a C4-C4 α double bond, a change that maintains the coplanarity of C4, N3, C4 α , and C5, as observed (Fig. 2, A and B). This observation is important because it explains, at least in PFORs, the role of C4 α , for which no function could be assigned previously (21).

All the models of the radical adduct of PFORs advanced so far have preserved the full aromaticity of the thiazole ring (Fig. 1B) (3, 12, 22–25), probably because a π -system in the ring has been traditionally considered essential for catalysis and even for cofactor integrity (21). However, if, as is generally accepted, the PFOR radical species corresponds to a reaction intermediate, our crystallographic results indicate that thiazole aromaticity is greatly reduced in this adduct and, consequently, the delocalization of the unpaired electron over this ring [the π -model (23, 26)] is extremely unlikely. Alternative models where the unpaired electron spin resides mostly in either the oxygen atom or in the C3 α of the substrate-derived group (Fig. 1B) have been put forward based on EPR experiments using either ¹³C-labeled (22, 23) or ²H-labeled pyruvate (12) or other 2-oxoacid substrates (3). In this respect, we observe that, for the two independent PFOR molecules in the asymmetric unit, the C2 α -C2 bond, connecting the acetyl group to the

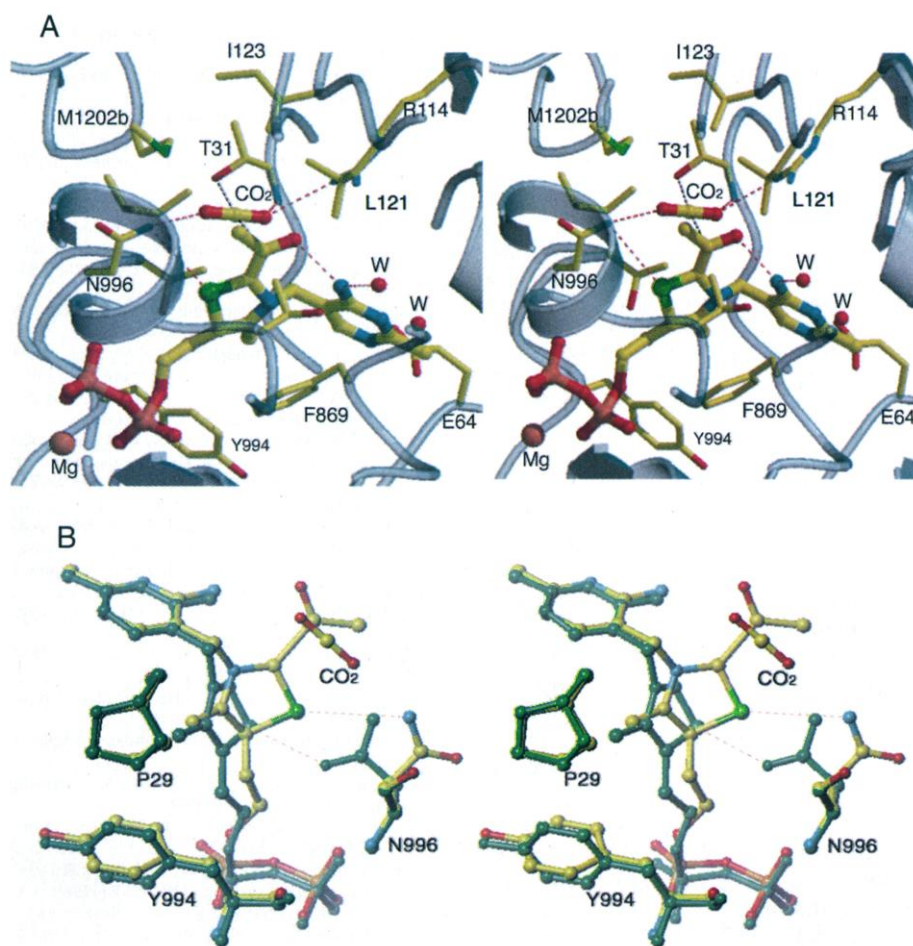
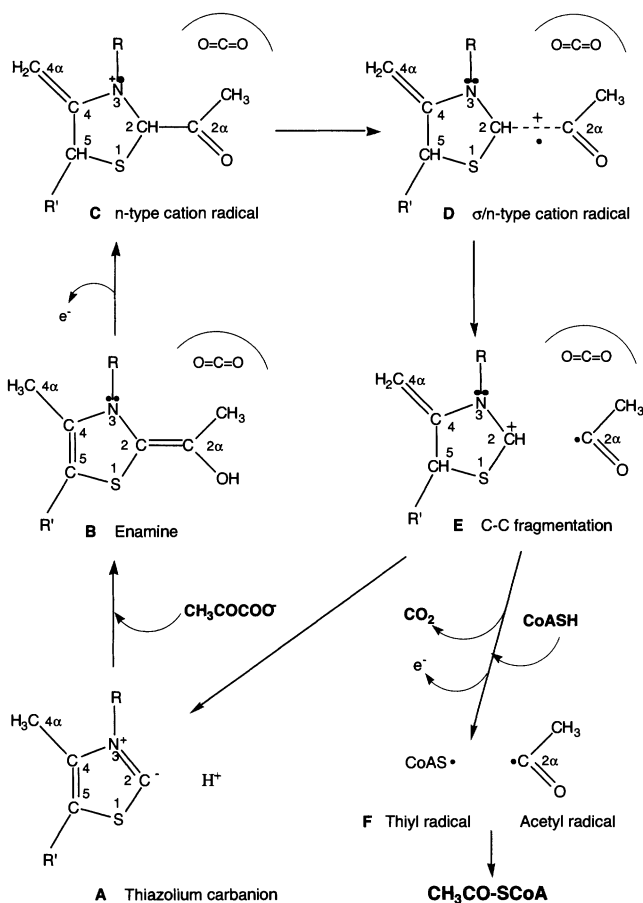


Fig. 3. (A) Stereo pair of the acetyl-ThDP moiety and the bound CO₂ molecule of PFOR and their protein environment. (B) Stereo pair of the superposition of a part of the active site of PFOR in the uncomplexed (green), and radical forms. The movements of the thiazole ring and the side chains of Asn⁹⁹⁶ and Tyr⁹⁹⁴ are concerted, and the S1 atom from the thiazole ring keeps its hydrogen bond to Asn⁹⁹⁶ in the two conformations. Part (A) was prepared using Molscript (39) and Raster3d (40); (B) was prepared with Turbo-Frodo (38).

Fig. 4. Postulated mechanism of acetyl-CoA synthesis by PFOR. Only the thiazolium ring moiety of ThDP is fully depicted (R and R' as in Fig. 1, B and C). (A) Deprotonated carbanion species (see Fig. 1A). The proton is putatively bound to 4'-iminopyridimine (not shown). (B) Pyruvate decarboxylation and hypothetical enamine formation; the CO₂ reaction product stays in the active site. (C) One electron transfer from the active site to one of the [4Fe4S] clusters. Hypothetical n cation radical formation. (D) Observed σ/n -type cation radical with a long C2-C2 α bond (27) and a bent thiazole ring (Fig. 2). Note that (i) ketonization of the enamine (B) upon radical formation (C) and (ii) tautomerization of the C5-C4 double bond to a C4-C4 α double bond, in going from (B) to (C), are required to explain the observed stereochemistry of the adduct. The net result of these two rearrangements is a significant reduction in the aromaticity of the thiazole ring. Because this process is generally considered to be unfavorable, the protein environment is thought to play a key role in the stabilization of (C) and (D). The loss of one electron from the active site and the bending of the thiazole ring are shown here as a single step because we do not know the detailed sequence of events. (E) Hypothetical fragmented C-C bond resulting in carbocation and acetyl radical species (28, 29). Upon fragmentation, the aromaticity of the thiazole ring is thought to be restored (A), closing the cycle. (F) Acetyl-CoA synthesis through condensation of a thiyl CoA radical with the acetyl radical. Although the reaction is shown in the direction of acetyl-CoA synthesis, PFORs are capable of catalyzing the reverse reaction.



thiazole ring, is refined to minimally restrained values of about 1.95 Å (molecule A) and 1.75 Å, (molecule B), instead of the expected distance of 1.54 Å for a single C-C bond. These long bonds are consistent with the omit electron density map and the crystallographically refined temperature factor parameters (Table 1 and Fig. 2). The observed C2 α -C2 bonds are reminiscent of the one-electron (long) bonds reported in cation radicals of vicinally difunctional molecules (27), a state intermediate in the fragmentation of C-C bonds into a carbocation and a radical species (28–30). Indeed, studies on the facile one-electron electrochemical oxidation of thiazole enamines strongly suggest that the radical species detected in PFORs could be a thiazolium cation radical. (31). If the observed long bonds have σ/n -type radical character (27), then the unpaired electron could be formally located at either the thiazole C2 or the substrate-derived C2 α (Figs. 1C and 4). Support for an acetyl radical such as

CH₃-C[•]=O in PFORs comes from ENDOR studies of the enzyme from *Clostridium thermoaceticum* (23) and its comparison with EPR studies on a trapped acetyl radical (32) [see (18) for a more elaborated discussion concerning the radical].

Taken together, the EPR and ENDOR data, the literature on long C-C bonds, and our own crystallographic results indicate that the unpaired electron is localized either at one or more atoms from the acetyl moiety or, less likely, at the C2 atom from the thiazole moiety but is significantly not delocalized over the thiazole ring. If an acetyl radical, or a related species, is in fact an intermediate state in the reaction, and given the description in hydrogenosomes of a CoA thiyl radical (22) and the report for several PFORs of reduction of one [4Fe4S] cluster by CoA, which could result in thiyl radical formation, (12, 25), the synthesis of acetyl-CoA by PFOR could take place via the condensation of an acetyl (PFOR-based) and a thiyl (CoA-based) radical species (12, 22). Radical chem-

istry in an anaerobic, ancient enzyme (3) would not be unexpected. Furthermore, it would highlight the versatility of ThDP as a cofactor capable of performing in aerobic, as well as anaerobic, environments through apparently different reaction mechanisms. Finally, our results indicate that the widespread description of the PFOR radical as an hydroxyethyl thiamine species is inappropriate and that an acetyl thiamine radical description, as the one used here, is the correct one.

References and Notes

- M. S. Patel, T. E. Roche, *FASEB J.* **4**, 3224 (1990).
- L. J. Reed, *Protein Sci.* **7**, 220 (1998).
- L. Kerscher, D. Oesterhelt, *Trends Biochem. Sci.* **7**, 371 (1982).
- M. C. W. Evans, B. B. Buchanan, D. I. Arnon, *Proc. Natl. Acad. Sci. U.S.A.* **55**, 928 (1966).
- A. Tersteegen, D. Linder, R. K. Thauer, R. Hedderich, *Eur. J. Biochem.* **242**, 862 (1997).
- G. D. Cody et al., *Science* **289**, 1337 (2000).
- G. Wächtershäuser, *Science* **289**, 1307 (2000).
- A. Kletzin, M. W. W. Adams, *J. Bacteriol.* **178**, 248 (1996).
- Q. Zhang, T. Iwasaki, T. Wakagi, T. Oshima, *J. Biochem. (Tokyo)* **120**, 587 (1996).
- R. Breslow, *J. Am. Chem. Soc.* **80**, 3719 (1958).
- G. Schneider, Y. Lindqvist, *Biochim. Biophys. Acta* **1385**, 387 (1998).
- S. Menon, S. W. Ragsdale, *Biochemistry* **36**, 8484 (1997).
- R. Cammack, L. Kerscher, D. Oesterhelt, *FEBS Lett.* **118**, 271 (1980).
- L. Pieulle et al., *Biochim. Biophys. Acta* **1250**, 49 (1995).
- A. Jordan, P. Reichard, *Annu. Rev. Biochem.* **67**, 71 (1998).
- P. A. Frey *Annu. Rev. Biochem.* **70**, 121 (2001).
- E. Chabrière et al., *Nature Struct. Biol.* **6**, 182 (1999).
- Supplementary material is available on Science Online at www.sciencemag.org/cgi/content/full/294/5551/2559/DC1.
- J. Stubbe, W. A. van der Donk, *Chem. Rev.* **98**, 705 (1998).
- We have previously reported a PFOR/pyruvate at pH 6.2 that appeared to have the substrate bound in a nonproductive way (17). However, it seems that this was a misinterpretation due to a possible pH drift toward more basic values caused by adding the pyruvate salt to the slightly buffered crystal-containing solution and/or the averaging of the nonequivalent electron density of the two molecules in the asymmetric unit. (We know now, as indicated in the text, that one of the molecules is more reactive; E. Chabrière, J. C. Fontecilla-Camps unpublished observations.)
- R. Breslow, *Ann. N.Y. Acad. Sci.* **98**, 445 (1962).
- R. Docampo, S. Moreno, R. Mason, *J. Biol. Chem.* **262**, 12417 (1987).
- V. F. Bouchev et al., *J. Am. Chem. Soc.* **121**, 3724 (1999).
- A. K. Bock, P. Schonheit, M. Teixeira, *FEBS Lett.* **414**, 209 (1997).
- E. T. Smith, J. M. Blamey, M. W. W. Adams, *Biochemistry* **33**, 1008 (1994).
- A. K. Bock, J. Kunow, J. Glasemacher, P. Schonheit, *Eur. J. Biochem.* **237**, 35 (1996).
- D. J. Bellville, R. A. Pabon, N. L. Bauld, *J. Am. Chem. Soc.* **107**, 4978 (1985).
- R. D. Burton, M. D. Bartberger, Y. Zhang, J. R. Eyler, S. S. Kirk, *J. Am. Chem. Soc.* **118**, 5655 (1996).
- P. Maslak, W. H. Chapman Jr., T. M. Vallombroso Jr., B. A. Watson, *J. Am. Chem. Soc.* **117**, 12380 (1995).
- This direct evidence of a long C-C bond in a biological system transcends the results reported here, because C-C fragmentation resulting from such bonds may occur even in the case of peptide bond cleavage (27).
- G. Barletta, A. C. Chung, C. B. Rios, F. Jordan, S. J. Schlegel, *J. Am. Chem. Soc.* **112**, 8144 (1990).
- J. E. Bennet, B. Mile, *Trans. Faraday Soc.* **67**, 1587 (1971).

33. X. Vernede, J. C. Fontecilla-Camps, *J. Appl. Crystallogr.* **32**, 505 (1999).
 34. Collaborative computational project, *Acta Crystallogr.* **D50**, 760 (1994).
 35. A. T. Brünger, *X-PLOR version 3.1: A System for X-ray Crystallography and NMR* (Yale Univ. Press, New Haven, CT, 1992).
 36. A. T. Brünger et al., *Acta Crystallogr.* **D54**, 905 (1998).
 37. D. Kern et al., *Science* **275**, 67 (1997).
 38. A. Roussel, C. Cambillaud, *Turbo-Frodo* (Silicon Graphics, Mountain View, CA, 1989), p. 77.
 39. P. J. Kraulis, *J. Appl. Crystallogr.* **24**, 946 (1991).
 40. E. A. Merritt, D. J. Bacon, *Methods Enzymol.* **277**, 505 (1997).
 41. We thank the staff of beamline ID-14 of the European Synchrotron Radiation Facility for help during data collection and S. Ragsdale, M. Fontecave, P. Amara, M. Field, and E. Mulliez for critical reading of the manu-

script. E.C. was the recipient of a fellowship from the French Ministry of Research. This work was supported by the Commissariat à l'Énergie Atomique and the CNRS. Coordinates and structure factors have been deposited in the Protein Data Bank, with accession code 1kek.

12 September 2001; accepted 2 November 2001

KLF6, a Candidate Tumor Suppressor Gene Mutated in Prostate Cancer

Goutham Narla,¹ Karen E. Heath,^{2*} Helen L. Reeves,^{1*} Dan Li,¹ Luciana E. Giono,¹ Alec C. Kimmelman,³ Marc J. Glucksman,^{4†} Jyothsna Narla,⁷ Francis J. Eng,¹ Andrew M. Chan,³ Anna C. Ferrari,^{3,5} John A. Martignetti,^{2,3,6} Scott L. Friedman^{1‡}

Kruppel-like factor 6 (*KLF6*) is a zinc finger transcription factor of unknown function. Here, we show that the *KLF6* gene is mutated in a subset of human prostate cancer. Loss-of-heterozygosity analysis revealed that one *KLF6* allele is deleted in 77% (17 of 22) of primary prostate tumors. Sequence analysis of the retained *KLF6* allele revealed mutations in 71% of these tumors. Functional studies confirm that whereas wild-type *KLF6* up-regulates p21 (*WAF1/CIP1*) in a p53-independent manner and significantly reduces cell proliferation, tumor-derived *KLF6* mutants do not. Our data suggest that *KLF6* is a tumor suppressor gene involved in human prostate cancer.

Prostate cancer is a leading cause of cancer death in men, with more than 198,000 new cases and 32,000 deaths annually in the United States alone. Loss of heterozygosity (LOH) analyses of sporadic prostate cancers and linkage studies of familial prostate cancer have provided strong evidence for the existence of prostate cancer-susceptibility genes (1). Although a number of tumor suppressor genes, including the retinoblastoma susceptibility gene (*RBI*), the putative protein tyrosine phosphatase gene (*P TEN*), and *p53*, have been implicated in prostate cancer, no single gene has yet been identified which is responsible for the majority of cases (2).

KLF6 (*Zf9/CPBP*) (GenBank accession number AF001461) is a ubiquitously ex-

pressed Kruppel-like transcription factor whose in vivo role has not been fully clarified (3–5). *KLF6* contains a proline- and serine-rich NH₂-terminal activation domain, and like other Kruppel-like factors, three COOH-terminal C2H2 zinc fingers. *KLF6* directly interacts with DNA through a GC box promoter element (3). Putative transcriptional targets of *KLF6* include the genes encoding a

placental glycoprotein (4), collagen $\alpha 1(I)$ (3), transforming growth factor $\beta 1$ (*TGF β 1*), types I and II *TGF β* receptors (6), urokinase type plasminogen activator (*uPA*) (7), and the human immunodeficiency virus long terminal repeat (*HIV-1 LTR*) (5).

The *KLF6* gene maps to human chromosome 10p, a region deleted in ~55% of sporadic prostate adenocarcinomas (8, 9). Given the role of Kruppel-like factors in the regulation of many cellular processes that include differentiation and development (10), we examined primary prostate tumor samples for specific LOH of the *KLF6* gene. Microsatellite markers flanking *KLF6* were analyzed in paired normal prostate tissue and in well to poorly differentiated prostate tumor specimens from 22 patients (11, 12). Of the 22 samples analyzed, 17 (77%) displayed LOH of the *KLF6* locus (Fig. 1A). To define the minimal region of loss, we designed two microsatellite markers, *KLF6M1* and *KLF6M2*, which flank the *KLF6* gene by ~42 kb and ~12 kb, respectively (12). Tumor DNA from patients 9 and 10 showed loss of only the tightly flanking *KLF6M1* and *KLF6M2* microsatellite markers, whereas that from patients 14 and 21 demonstrated loss of only *KLF6M1* (Fig. 1A). Representative fluorescent electropherograms for microdissected tumor samples with loss of *KLF6M1* are shown in Fig. 1B.

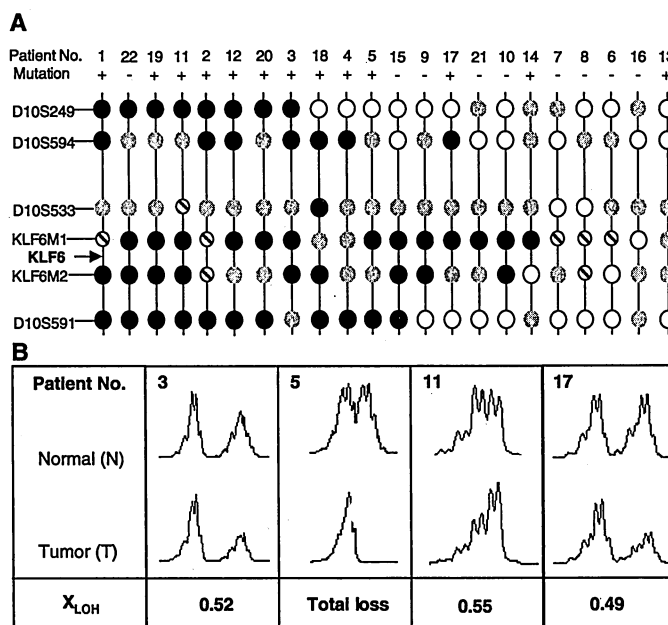


Fig. 1. LOH at the *KLF6* locus in human prostate tumors. (A) Summary of LOH patterns of 22 prostate tumors. Retained microsatellite markers are indicated in white, markers demonstrating allelic loss in black, and noninformative markers in gray. A hatched circle indicates DNA that could not be amplified. Patient data was grouped according to degree of LOH. Genetic map is not drawn to scale. (B) Representative fluorescent electropherograms for microsatellite marker *KLF6M1* for patients with LOH. A X_{LOH} score of less than 0.7 was used for determination of LOH (12).

¹Division of Liver Diseases, Department of Medicine, ²Department of Human Genetics, ³The Derald H. Rutenber Cancer Center, ⁴Department of Neurobiology, ⁵Division of Medical Oncology, Department of Medicine, and ⁶Department of Pediatrics, Mount Sinai School of Medicine, 1425 Madison Avenue, Room 1170F, Box 1123, New York, NY, 10029, USA. ⁷Regional Medical Center, 225 North Jackson, San Jose, CA, 95116, USA.

*These authors contributed equally to this work.
 †Present address: Structural Neurobiology and Proteomics Laboratory, Department of Biochemistry and Molecular Biology, FUHS/Chicago Medical School, 3333 Green Bay Road, North Chicago, IL 60064, USA.
 ‡To whom correspondence should be addressed. E-mail: friedso2@doc.mssm.edu